Al-Nahrain Journal for Engineering Sciences **NJES** 25(1)49-54, 2022
http://doi.org/10.29194/NJES.25010049

Vibration Characteristics of the Bearing Rotor Shaft

Karrar Baher[1], Qasim A. Atiyah[2], Imad A. Abdulsahib[3]

Authors affiliations:
1) Mechanical Engineering Department, University of Technology, Baghdad, Iraq.
me.19.20@grad.uotechnology.edu.iq

2) Mechanical Engineering Department, University of Technology, Baghdad, Iraq.
20044@uotechnology.edu.iq

3) Mechanical Engineering Department, University of Technology, Baghdad, Iraq.
20018@uotechnology.edu.iq

Paper History:

Received: 12th Dec. 2021

Revised: 29th Dec. 2021

Accepted: 2nd March 2022

Abstract

In this work, the vibrations in the rotor-bearing system are studied experimentally and theoretically using ANSYS Workbench 2020 R1 software to compute the natural frequencies and mode shapes. In the experimental part, the LABVIEW software was used to examine the signal of the frequency domain values obtained from the accelerometer sensors, based on Fast Fourier Transform (FFT) technology and dynamic response spectrum. in the theoretical part, the natural frequencies are determined based on the finite element method for analyzing the system and knowing its behavior and vibration response level. The results showed that the level of vibration becomes higher at high rotational speeds, and it becomes large when the distances between the bearings are large, according to the bearing position and type used in the system. in this work can be concluded, the system is usually affected by the dynamic response around it and is difficult to separate from it, and the vibrations in the system can be controlled by adding an external damping source, which gives the system more stable. A system operating at high speeds can give a large vibration and an unbalanced response.

Keywords: Vibrations, Ball Bearing, Fast Fourier Transform (FFT), Natural Frequency, Rotor-Bearing System, ANSYS, LABVIEW, Dynamic Response, Modes Shapes.

خصائص الاهتزاز لعمود الدوران مع المحمل

كرار باهر، قاسم عباس عطية، عماد عبد الحسين عبد الصاحب

الخلاصة:

في هذا العمل، تمت دراسة الاهتزازات في النظام المحمل الدوار تجريبيًا ونظريًا باستخدام برنامج ANSYS Workbench 2020 R1 لحساب الترددات الطبيعية وأشكال الوضع. في الجزء التجريبي، تم استخدام برنامج LABVIEW لفحص إشارة قيم مجال التردد التي تم الحصول عليها من مستشعرات مقياس التسارع، بناءً على تقنية تحويل فورييه السريع (FFT) وطيف الاستجابة الديناميكي. في الجزء النظري، يتم تحديد الترددات الطبيعية بناءً على طريقة العناصر المحدودة لتحليل النظام ومعرفة سلوكه ومستوى استجابة الاهتزاز. أظهرت النتائج أن مستوى الاهتزاز يصبح أعلى عند سرعات الدوران العالية، ويصبح كبيرًا عندما تكون المسافات بين المحامل كبيرة وفقًا لموضع المحمل والنوع المستخدم في النظام. في هذا العمل يمكن استنتاج أن النظام يتأثر عادة بالاستجابة الديناميكية من حوله ويصعب فصله عنها، ويمكن التحكم في الاهتزازات في النظام عن طريق إضافة مصدر التخميد الخارجي، مما يعطي النظام أكثر استقرارًا. يمكن أن يعطي النظام الذي يعمل بسرعات عالية اهتزازًا كبيرًا واستجابة غير متوازنة..

List of symbols

I	Area moment of inertia (m^4)
q_{2i-1}	Transverse deflection (m)
q_{2i}	Rotation (Slope) (m)
α_i	Constant
$[N]$	Shape functions matrix
$N(x)$	Nodal interpolation functions
u	Axial displacement (m)

NJES is an **open access Journal** with **ISSN 2521-9154** and **eISSN 2521-9162**

v	Transverse displacement (m)
γ	Distance from the neutral axis (m)
$[M]_e$	Global mass matrix (Kg)
$[K]_e$	Global stiffness matrix (N/m)
E	Young's modulus (Pa)
L	Length of beam (m)
m	Mass (Kg)
$[K]$	Stiffness matrix (N/m)
$[M]$	Mass matrix (Kg)
ω_n	Natural frequency (rad/s)

1. Introduction

Vibrations are a natural occurrence in rotating machinery. They can be found in a wide variety of machines and mechanical pieces. They are undesirable since they conflict with the optimum output of these components, and hence must be removed [١]. Vibration issues have become more common with the rapid growth of the rotordynamic Machines. These concerns pose a major challenge to both safety production and economic gains. Rotor structures vibrate frequently in machinery due to unbalance, resulting in impeller rupture, seal loss, bearing destroy, valve failure, pipeline leakage, and loose primer. These vulnerabilities result in equipment failure or even significant safety incidents [2, 3]. Many industrial applications use rigid rotor systems assisted on linear or nonlinear elastic bearings, such as onboard space vehicles, revolving machinery in electrical power plants, and power transmission gear trains, among others. As a result, modeling and understanding their complex behavior has become a major research subject, and the fundamental theory is now well developed [4, 5].

2. Previous Work

Researchers have contributed greatly to the study of vibrations and ways to reduce them, with most of them providing various means to explore and analyze the dynamic response of the rotor and bearings on which it is supported. Isaksson [6] concluded that stator stiffness managed by the springs could improve the system's stability. Tiwari et al. [7] suggested a deep-groove ball bearing model that takes the clearance and Hertzian contact feature into consideration. The influence of bearing forces on the geometrical interaction of the bearing elements on the other hand, was not taken into account. Qin et al. [8] examined the dynamic reaction of a rotor rubbing against an outer casing. A horizontal overhung rotor was mounted on a stepped hollow shaft backed by two journal bearings and surrounded by an outer ring in the physical model. The investigation concluded that raising the stiffness of the support will delay the occurrence of rubbing, resulting in a high critical speed, using the transfer matrix process. Chu and Lu [9] investigated into the rotor's stiffening effect during the rotor-to-stator interaction. It was discovered that during the rub-impact, the natural frequencies of the device experience a transient dynamic change, reflecting the rotor stiffening effect. Ghafari et al. [10] proposed a nonlinear dynamic model for the balanced defect-free ball bearing based on the Hertzian contact deformation principle. They discovered that as bearing clearance expanded, the equilibrium points of the bearing bifurcated into a supercritical pitchfork. The dynamic study of a harmonically excited on-board rotor-bearing device was described by Dakel et al. [11]. Babu et al. [12] suggested an empirical model of a rigid rotor assisted on two angular contacts deep groove ball bearing. The authors discovered that the bearing load has a substantial impact on the effect of frictional moment on device vibration. Zhang et al. [13] established a rotor ball bearing device computational formula determining the effect of unbalanced force on bearing stiffness. Jalali et al. [14] developed a three-dimensional finite element analysis of a high-speed rotor with specific mechanical and geometrical characteristics. They calculated the rotor's mode shapes and natural frequency in field condition. In another study, Zhang et al. [15] investigated at the difference of contact angle in addition to the disbalance effect of the load. Under time-periodic core angular movements, Han et al. [16] identified the parametric imbalance of a dynamic rotor-bearing device. Meng et al. [17] examined the balance of an asymmetric anisotropic system. They described the rotor using 3D solid components, which makes for more precise prediction of rotors with complicated shape. The diminished linear model is more reliable and time effective than measured data, and it can be used in a variety of practical research papers.

This study deals with the dynamics of the rotor-bearing system, and aims to explore the rotor response and Mode Shapes depending on the change of the number of nodes using the Finite Element Analyzes. It is based on Fast Fourier Transform (FFT) and LABVIEW software to find the Mode Shapes of the rotating bearing.

3. Theoretical Model

A rotary shaft can be modeled as a beam. The distorted geometry of a beam is characterized by the transverse motion and slope, provided the beam is symmetric around the y and z axes. As a result, the unexplained degrees of freedom are the transverse movement and rotations at either end of the beam element. The four degrees of freedom in the localized (x-y) coordinate system are denoted as q_1, q_2, q_3, and q_4 for a beam element of length l located in the x-y plane, as shown in Figure (1). A polynomial function for v(x) was assumed, as there are four nodal deflections (Figure (1)) [18, 19].

$$v(x) = \alpha_1 + \alpha_2 x + \alpha_3 x^2 + \alpha_4 x^3 \quad (1)$$

utilizing the requirements to find the constants $\alpha_1$to α_2 .

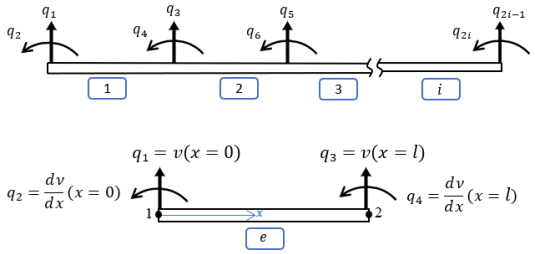

Figure. (1): Beam Element with Degrees of Freedom.

$$v(x) = q_1 \text{ and } \frac{\mathrm{d}v}{\mathrm{d}x}(x) = q_2 \text{ at } x = 0$$

$$v(x) = q_3 \text{ and } \frac{\mathrm{d}v}{\mathrm{d}x}(x) = q_4 \text{ at } x = l$$

As a result equation (1) can be written as

$$\underset{1\times1}{v(x)} = \underset{1\times4}{[N]} \quad \underset{4\times1}{\vec{q}} \tag{2}$$

Where, matrix of shape functions [N] is equal to

$$[N] = [N_1 \quad N_2 \quad N_3 \quad N_4] \tag{3}$$
$$N_1(x) = (2x^3 - 3lx^2 + l^3) / l^3 \tag{4}b$$
$$N_2(x) = (x^3 - 2lx^2 + l^3x) / l^2 \tag{4}c$$
$$N_3(x) = -(2x^3 - 3lx^2) / l^3 \tag{4}d$$
$$N_4(x) = (x^3 - lx^2) / l^2 \tag{4}e$$

Where, $N_i(x)$ is nodal interpolation functions

$$\vec{q} = \begin{Bmatrix} q_1 \\ q_2 \\ q_3 \\ q_4 \end{Bmatrix} \tag{5}$$

The axial displacement u caused by the transverse displacement v can be stated in the following way.

$$u = -\gamma \frac{\partial v}{\partial x} \tag{6}$$

The distance from the neutral axis is denoted by the letter γ. The stiffness matrix is as follows:

$$[\mathrm{K}]_\mathrm{e} = \frac{EI}{L^3} \begin{bmatrix} 12 & 6l & -12 & 6l \\ 6l & 4l^2 & -6l & 2l^2 \\ -12 & -6l & 12 & -6l \\ 6l & 2l^2 & -6l & 4l^2 \end{bmatrix} \tag{7}$$

between nodes 1 and 2, is the element stiffness matrix

$$[\mathrm{M}]_\mathrm{e} = \frac{\mathrm{mL}}{420} \begin{bmatrix} 156 & 22\mathrm{L} & 54 & -13\mathrm{L} \\ 22\mathrm{L} & 4\mathrm{L}^2 & 13\mathrm{L} & -3\mathrm{L}^2 \\ 54 & 13\mathrm{L} & 156 & -22\mathrm{L} \\ -13\mathrm{L} & -3\mathrm{L}^2 & -22\mathrm{L} & 4\mathrm{L}^2 \end{bmatrix} \tag{8}$$

where m is the mass per element length and is the element inertia matrix.

Relying on the continuous system using the finite element method and for a non-trivial solution, the following formula for calculating the natural frequency is obtained:

$$[[K] - \omega_n^2[M]] = 0 \tag{9}$$

4. Experimental Work

4.1 Material Characteristics

Ck45 alloy steel was used in the manufacture of the shafts used in the system. Alloy steel Ck45 is one of the best common types used in industrial applications, and it is considered one of the medium iron alloys that contain carbon, where the ratio ranges approximately (0.42 - 0.50) according to British Standard No. [10083 - 2 - 2006 - 08 Table No. 3]. Chromium Steel has been used in the block of linear ball bearing and linear sliding rail due to its outstanding operational characteristics.

4.2 Accelerometer Sensor

The ADXL335 accelerometer sensor was used to measure acceleration in a rotating bearing system, it is a full 3-axis accelerometer with a signal modal voltage output that is compact, thin, and low power consumption. The instrument monitors acceleration across a whole range of 3g. It can detect both static and dynamic gravity acceleration in tilt sensors due to continuous motion, shocks, or vibrations. The bandwidth of the X and Y axes can range from 0.5 Hz to 1600 Hz, while the bandwidth of the Z axis can range from 0.5 Hz to 550 Hz.

Acceleration signals were converted into frequency field values using Fast Fourier Transform (FFT) technique, by entering the signal into the LabVIEW program to get the frequencies resulting from the vibration of the bearing-rotor system.

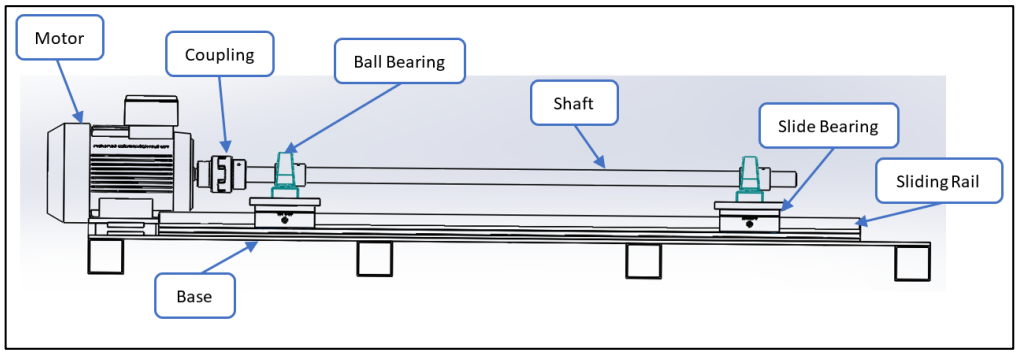

Figure. (2): Test Rig.

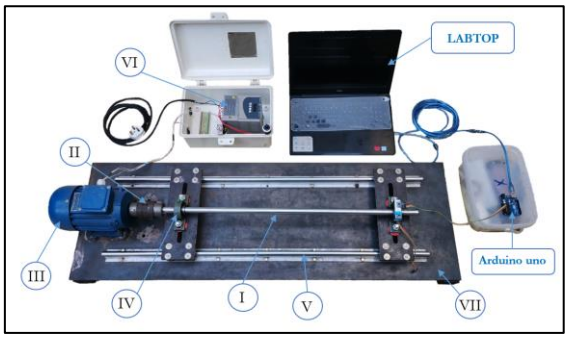

Figure. (3): Experimental Rig.

The main components of the system in this work are:

I. The rotating shaft is 80 cm long and 20 mm in diameter and made of AISI 1045 Carbon Steel.

II. Coupling of iron metal and the inner cavity on the motor and shaft side 14 and 20 mm respectively.

III. A motor with a rotational speed of 3000 rpm, a voltage of 220 / 380 volts and a current of 1.7 / 0.99 amps.

IV. ball bearing with an inner diameter of 20 mm.

V. Linear Sliding Rail and Linear Ball Bearing Block to control the distance between the bearings.

VI. AC type rotary speed converter

VII. The base is made of iron, with a length of 120 cm, a width of 40 cm, and a thickness of 5 mm.

5. Results and discussion

The natural frequencies were calculated using the finite element method for a different number of nodes. It was relied on equation (9) after finding the stiffness and mass matrices, and applying the global matrix for a number of nodes, for fourteen elements, satisfactory results were reached in accordance with exact methods [19]. In Table (1), the comparison ratio between the finite element method and exact method was found, and the difference rate was found. The concordance of the values in the two methods is noted, which indicates accuracy.

Table (1): The frequencies of uniform beams by Finite Elements - exact methods:

No. Nodes	*Finite element Method (HZ)*	*Exact Method (HZ) [19]*	*Difference %*
5 - Nodes	*67.463*	*62.524*	*7.321*
7 - Nodes	*66.925*	*62.540*	*6.552*
9 - Nodes	*66.354*	*62.564*	*5.712*
12 - Nodes	*65.948*	*62.569*	*5.123*
15 - Nodes	*65.853*	*62.653*	*4.859*

Figure (4) shows the value of the frequencies using the finite element method for a given number of degrees of freedom. Which indicates that after the first five nodes, the values begin to remain stable. For example, after using the fifteen nodes, the values are almost constant. Which gives an indication of the accuracy reached using this method. No tilt is observed in the continuous line of frequencies after the first values are exceeded.

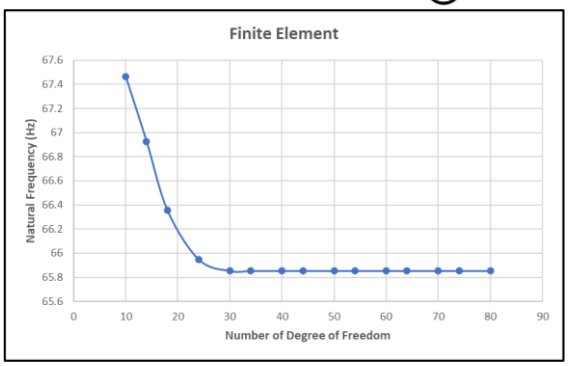

Figure (4): Frequencies of Finite Elements for number of degrees of freedom.

5.1 Numerical Aspect by ANSYS

The ANSYS simulation program analyzes the system in this work. Where the rotating shaft is treated as a simply supported beam. Varied mode shapes are obtained using the ANSYS program, as shown in Figure (6), which shows the different mode shapes of the shaft because of the speed difference, with six mode shapes listed. The Campbell diagram is extracted from the results obtained numerically from the program and is illustrated in Figure (5). The figure shows the stability of the rotation of the rotating shaft during the operation of the system thru five rotational speeds.

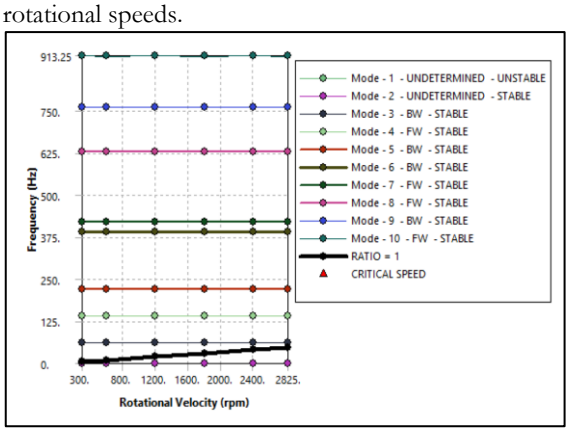

Figure (5): Mode shape of simply supported beam.

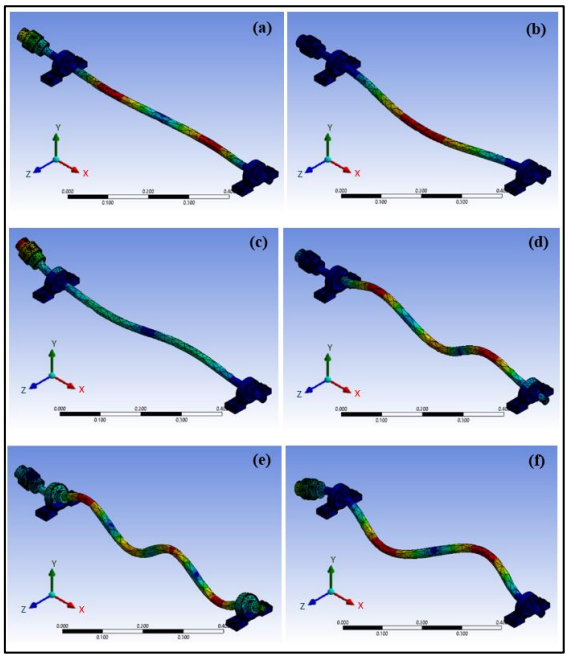

Figure (6): Mode shape of simply supported beam by ANSYS (a) 1st mode shape (b) 2nd mode shape (c) 3rd mode shape (d) 4th mode shape (e) 5th mode shape (f) 6th mode shape.

As for the mesh details of the components, the default size of the program was relied upon, as shown in Figure (7), and it was as follows: bounding box diagonal length 0.86636 m, average surface area 1.7176e-004 m², and minimum edge length 4.1385e-005 m. For the inflation option, the transition ratio was 0.272, the maximum layer was 5, and the growth rate was 1.2.

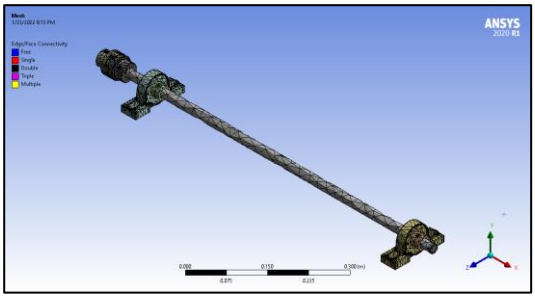

Figure (٧): Mesh of simply supported beam by ANSYS

In Table (2), the first five natural frequencies were compared between the numerical side by ANSYS with the experimental side. It turns out that the values of the first natural frequencies are close to a large extent, and this gives greater reliability.

In Figure (٨) the vibrations of the rotating shaft in the case simply supported beam, shown in a simple schematic diagram in Figure (6), were studied for the vertical Z axis using LabVIEW software, where it was observed that the value of the natural frequency starts at 65 Hz, and this is the value of the first critical frequency for this position, and the value of the second natural frequency is fixed at 125 Hz and the third becomes 200 Hz. It is compared with the frequencies extracted numerically using the ANSYS program, and the large convergence of the values is noted, which gives greater reliability and accuracy of the work.

Table (2): Comparison of natural frequencies experimentally and numerically by ANSYS:

No. of Natural Frequency	Experimental (HZ)	Numerical (HZ)	Difference %
1st	5.013	60.762	6.996
2nd	125.845	141.88	11.302
3rd	200.246	220.82	9.317
4th	380.856	389.94	2.329
5th	440.218	420.77	4.622

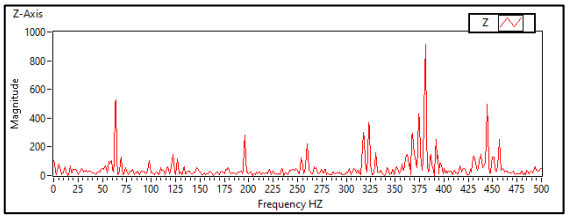

Figure (8): Natural frequency of rotor by LABVIEW program.

6. Conclusion

The system is usually affected by the dynamic response around it and is difficult to separate from it, and special vibrations in the system can be controlled by adding an external damping source, which gives the system more stability. A system operating at high speeds can give a large vibration and an unbalanced response. The conclusions obtained can be summarized in the following points:

1- At low speeds a quasi-stable level of vibration are get and these vibration levels start to rise at high speeds.

2- The greater the number of nodes in the mathematical calculations, gives the greater accuracy of the results obtained, until they begin to stabilize at a certain number of nodes and reach the exact value.

3- Vibrations can be greatly affected by changing the position of the bearings and by changing the distance between the bearings. When the distances between the bearings become wide, it gives greater values of natural frequencies, which negatively affects the system.

4- Bearing clearance affects the dynamic response and the level of vibrations, when the amount of clearance in the bearings increases, it leads to imbalance of the system.

5- External dampers can be added to the system and to obtain stability in the rotation of the shaft as a solution to reduce the level of vibrations.

7. References:

[1] G. Chandrashekar, W. Raj, C. Godwin, and P. S. Paul, "Study On The Influence Of Shaft Material On Vibration In Rotating Machinery," Materials Today: Proceedings, vol. 5, no. 5, pp. 12071-12076, 2018, doi: 10.1016/j.matpr.2018.02.182.

[2] Q. Jiang, L. Zhai, L. Wang, and D. Wu, "Fluid-structure interaction analysis of annular seals and rotor systems in multi-stage pumps," Journal of Mechanical Science and Technology, vol. 27, no.

7, pp. 1893-1902, 2013/07/01 2013, doi: 10.1007/s12206-013-0507-y.

[3] Y. Zhang, L. He, J. Yang, F. Wan, and J. Gao, "Vibration Control of an Unbalanced Single-Side Cantilevered Rotor System with a Novel Integral Squeeze Film Bearing Damper," Applied Sciences, vol. 9, no. 20, 2019, doi: 10.3390/app9204371.

[4] F. M. A. El-Saeidy and F. Sticher, "Dynamics of a Rigid Rotor Linear/Nonlinear Bearings System Subject to Rotating Unbalance and Base Excitations," Journal of Vibration and Control, vol. 16, no. 3, pp. 403-438, 2009, doi: 10.1177/1077546309103565.

[5] A. H. Haslam, C. W. Schwingshackl, and A. I. J. Rix, "A parametric study of an unbalanced Jeffcott rotor supported by a rolling-element bearing," Nonlinear Dynamics, vol. 99, no. 4, pp. 2571-2604, 2020, doi: 10.1007/s11071-020-05470-4.

[6] J. L. Isaksson, Dynamics of rotors influenced by rubbing contacts. Division of Machine Design, Department of Mechanical Engineering, Linköping …, 1997.

[7] M. Tiwari, K. Gupta, and O. Prakash, "Dynamic response of an unbalanced rotor supported on ball bearings," Journal of sound and vibration, vol. 238, no. 5, pp. 757-779, 2000.

[8] W. Qin, G. Chen, and G. Meng, "Nonlinear responses of a rub-impact overhung rotor," Chaos, Solitons & Fractals, vol. 19, no. 5, pp. 1161-1172, 2004.

[9] F. Chu and W. Lu, "Stiffening effect of the rotor during the rotor-to-stator rub in a rotating machine," Journal of Sound and vibration, vol. 308, no. 3-5, pp. 758-766, 2007.

[10] S. Ghafari, E. Abdel-Rahman, F. Golnaraghi, and F. Ismail, "Vibrations of balanced fault-free ball bearings," Journal of Sound and Vibration, vol. 329, no. 9, pp. 1332-1347, 2010.

[11] M. Z. Dakel, S. Baguet, and R. Dufour, "Dynamic analysis of a harmonically excited on-board rotor-bearing system," in 10th IMechE International Conference on Vibrations in Rotating Machinery (VIRM10), 2012, p. C1326/024.

[12] C. Babu, N. Tandon, and R. Pandey, "Vibration modeling of a rigid rotor supported on the lubricated angular contact ball bearings considering six degrees of freedom and waviness on balls and races," Journal of Vibration and Acoustics, vol. 134, no. 1, 2012.

[13] X. Zhang, Q. Han, Z. Peng, and F. Chu, "Stability analysis of a rotor–bearing system with time-varying bearing stiffness due to finite number of balls and unbalanced force," Journal of Sound and Vibration, vol. 332, no. 25, pp. 6768-6784, 2013.

[14] M. H. Jalali, M. Ghayour, S. Ziaei-Rad, and B. Shahriari, "Dynamic analysis of a high speed rotor-bearing system," Measurement, vol. 53, pp. 1-9, 2014.

[15] X. Zhang, Q. Han, Z. Peng, and F. Chu, "A new nonlinear dynamic model of the rotor-bearing system considering preload and
varying contact angle of the bearing," Communications in Nonlinear Science and Numerical Simulation, vol. 22, no. 1-3, pp. 821-841, 2015.

[16] Q. Han and F. Chu, "Parametric instability of flexible rotor-bearing system under time-periodic base angular motions," Applied Mathematical Modelling, vol. 39, no. 15, pp. 4511-4522, 2015.

[17] M. W. Meng, W. J. Jun, and W. Zhi, "Frequency and stability analysis method of asymmetric anisotropic rotor-bearing system based on three-dimensional solid finite element method," Journal of Engineering for Gas Turbines and Power, vol. 137, no. 10, 2015.

[18] S. S. Rao, The finite element method in engineering. Butterworth-heinemann, 2017.

[19] S. S. Rao, "Mechanical Vibrations, in SI Units, Global Edition," ed: Pearson, London, 2017.